https://doi.org/10.5194/amt-2024-163
Preprint. Discussion started: 1 October 2024

Atmospheric Measurement Techniques Discussions

Effectiveness of Cirrus Detection with MODIS Cloud Mask data

Żaneta Nguyen Huu[1,2], Andrzej Z. Kotarba[3], and Agnieszka Wypych[1]

[1]Institute of Geography and Spatial Management, Jagiellonian University, 7 Gronostajowa St, 30-387 Kraków, Poland
[2]Jagiellonian University, Doctoral School of Exact and Natural Sciences, Prof. St. Łojasiewicza St 11, PL30348, Cracow, Poland
[3]Space Research Centre, Polish Academy of Sciences, Bartycka 18A, 00-716 Warsaw, Poland

Correspondence: Żaneta Nguyen Huu (zaneta.nguyen_huu@uj.edu.pl)

Abstract. All clouds influence the Earth's radiative budget, with their net radiative forcing being negative. However, high-level clouds warrant special attention due to their atmospheric warming effects. A comprehensive characterization of cirrus requires information on cloud coverage, obtainable from various data types. Active satellite sensors are presently the most accurate source for cirrus data, but their usefulness in climatological studies is limited. On the contrary, passive data, available for the past 40 years with sufficient temporal resolution for climatological research, were not specifically designed for cirrus detection. In this study, we assessed the utility of MODIS standard products for creating a cirrus mask by validating them against CALIOP data. Our objective was to determine if a MODIS product exists that detects cirrus with the same accuracy as CALIOP.

Using CALIOP data as the reference, we evaluated six tests for cirrus detection considered in MODIS cloud masking algorithm and their combination (ALL TESTS CONSOLIDATION, ATC). Additionally we applied two ISCCP-originating tests: ISCCP3.6 and ISCCP23 tests. All tests have been applied to MODIS radiances.

Study revealed that ATC test was the most effective resulting with the overall accuracy of 72.98% during daytime and 59.50% at night (probability of detection: 80.87% and 25.46%, false alarm rate of 34.86% and 6.90%, and Cohen's kapppa coefficient of 0.46 and 0.19 respectively). However, its effectiveness was notably reduced during nighttime compared to daytime. We conclude that the test is suitable for creating a mask of high-level clouds.

https://doi.org/10.5194/amt-2024-163
Preprint. Discussion started: 1 October 2024

Atmospheric Measurement Techniques Discussions

1 Introduction

Clouds are indispensable to Earth's environmental systems and human life, influencing weather, climate, water distribution, ecosystems, and various human activities. All of them affect the Earth's radiative budget, and their net radiative forcing for is negative and equal to -13 Wm-2 (Ramanathan et al., 1989). That means that clouds, in general, cools the atmosphere. Nevertheless a special attention should be paid to high-level clouds (according to WMO, high-level clouds include all types of Cirrus, Cirrocumulus, and Cirrostratus clouds. Additionally, clouds resulting from anthropogenic activities, such as aviation contrails, are classified within the high-level cloud category (WMO, 1977)) named with the customary term cirrus. Cirrus clouds have a complex role in climate regulation. The relation between cirrus particles (size, shape and albedo) and Earth's radiation budget has been examined (Kinne and Liou, 1989; Macke et al., 1998; Mishchenko et al., 1996; Stephens et al., 1990; Zhang et al., 1994, 1999), resulting in a general conclusion that cirrus play an important role and can warm the atmosphere. Cirrus typically have a base above about 8 000 metres and are composed of small particles – ice crystals. Because of cirrus specific properties (cloud height, temperature, effective particle size, surface thermal contrast, ice water path and cloud optical depth; Ackerman et al. (1988); Stephens et al. (1990); Stephens and Webster (1981)), in contrast to low- and mid-level clouds, they heat the Earth (they allows shortwave radiation to reach Earth's surface and reduces outgoing longwave radiation). Recent research shows that cirrus radiative forcing varies from about 0.05 Wm-2 for contrails, to 35.5 Wm-2 for cirrus in general (Bock and Burkhardt, 2016; Campbell et al., 2016; Kärcher, 2018; Lolli et al., 2017; Oreopoulos et al., 2017). Additionally, their presence change the radiative forcing of other clouds for positive as well. For instance, when medium and low clouds co-occur, their radiative effect equals -18.8 Wm-2. Additional presence of cirrus raises the radiative effect to 50,8 Wm-2 (Oreopoulos et al., 2017).

Cirrus properties description is incomplete without the information about cloud coverage. Most of the studies, have considered just a total cloud cover, but some of them also study high-level cloudiness. The global frequency of cirrus occurrence is between 28% and 42% . Research conducted using high resolution satellite data has shown that global cloud coverage is estimated at about 66% to 74% and 40% of all clouds are high-level clouds (Stubenrauch et al., 2010). According to Sassen et al. (2008) cirrus cover almost 17% of Earth's surface. The study of high-level cloud coverage and its trends has long intrigued scientists. In 1994, Wylie et al. presented global statistics on cirrus clouds over a four-year period, revealing an average cirrus coverage of 42% based on HIRS data. More recently, Li and Groß (2022) analyzed a decade of CALIPSO lidar measurements, finding that cirrus clouds over Europe occur most frequently between 9 to 11 km altitude, with occurrence rates varying seasonally from about 5% in summer to 12% in winter. Another significant study used 16 years of ISCCP data to identify trends in cirrus clouds across Europe, noting an increase of 1-2% per decade in regions with high aircraft traffic, contrasting with a general decline elsewhere (Stordal et al., 2005). A 16-year ground-based lidar study in Gadanki, India, observed peak cirrus occurrence at 14.5 km with a 25% frequency (Pandit et al., 2015). The most extended study, spanning 20 years (1983-2004) with ISCCP data, documented high cirrus concentrations in regions such as the South Pacific Convergence Zone, the Amazon, and central Africa, while noting a global decrease in cirrus clouds except in the southern mid-latitudes, where no significant trend was observed (Eleftheratos et al., 2007). Numerous studies have explored changes in high-level cloud coverage. However, those

https://doi.org/10.5194/amt-2024-163
Preprint. Discussion started: 1 October 2024


Atmospheric Measurement Techniques Discussions

relying on satellite data often lack a focus on cirrus clouds over sufficiently long periods—at least 30 years, as recommended by the WMO. Conducting such studies and identifying suitable data sources pose significant challenges.

Given the critical role of cloud cover, especially cirrus clouds, in atmospheric studies, the observation of clouds is considerably significant. Historically first method is visual observation from ground-based meteorological stations, which is simple and provides long time series data. However, this method has limitations, including difficulty in detecting high-level clouds due to cloud overlap at multiple altitudes, perspective issues near the horizon, and the optical thinness of cirrus clouds. Studies have shown that under optimal conditions, the probability of detecting cirrus clouds visually ranges from 44% to 83% during the day and 24% to 42% at night. With clouds at all levels, detection probabilities drop to 47%–71% during the day and 28%–43% at night (Kotarba and Nguyen Huu, 2022).

Present cloud climatologies benefit from satellite remote sensing. Initially, this information was obtained from various imagers, sounders, and radiometers, which utilize passive cloud detection methods (involving detecting natural radiation emitted or reflected by objects, such as clouds, without actively sending out signals). Researchers such as Ackerman et al. (2008); Amato et al. (2008); Chen et al. (2002); Frey et al. (2008, 2020); Gu et al. (2011); Kotarba (2016); Liu et al. (2004); Minnis et al. (2008); Murino et al. (2014); Musial et al. (2014); Tang et al. (2013) have contributed to these studies. An example of passive utensil can be MODIS (Moderate Resolution Imaging Spectroradiometer), which is a key instrument aboard the Terra and Aqua satellites.

Active remote sensing technology relies on its own signal, directing it at an object and analyzing the response. This allows active sensors, in example CALIPSO's (Cloud-Aerosol Lidar and Infrared Pathfinder Satellite Observations) lidar, CALIOP (Cloud-Aerosol Lidar with Orthogonal Polarization), to operate day and night with similar efficiency. Active profiling instruments like CALIOP, which provide high-resolution vertical profiles of aerosols and clouds, have limitations such as a narrow field of view. This narrow view, combined with a long 16-day repeat cycle, results in only about 20 observations per year of the same region, which is challenging and sometimes insufficient for climatological studies.

Although active sensors, like CALIOP, are currently the best source of cirrus data (Heidinger and Pavolonis, 2009), their potential for construing long-term climatologies is very limited. On the contrary, passive data are available for last more than 40 years with good enough for climatological research time resolution (i.e. for MODIS we have access to over 20 years of data), although they were not designed for cirrus detection. In this paper, we examined utility of MODIS products to create a cirrus mask by validating them with CALIOP data. Our objective is to determine whether any existing operational MODIS product detect cirrus clouds as accurately as the CALIPSO does. Specifically, we aim to assess whether MODIS Cloud Mask, when examining its individual tests could be easily adapted into an algorithm for masking cirrus clouds. We also seek to identify the conditions under which this approach would be effective and when it might not be suitable.

2 Data and methods

In this study, we use active data for validating passive-based information for determining the presence of cirrus. The active dataset was collected by the CALIOP lidar aboard the CALIPSO satellite, while the passive data was obtained from the MODIS

https://doi.org/10.5194/amt-2024-163
Preprint. Discussion started: 1 October 2024


Atmospheric Measurement Techniques Discussions

spectroradiometer on the Aqua satellite. The concept behind achieving the research objective was based on collocation those two datasets in time and space. Data for the year 2015 were analyzed for the whole globe. These include 136,272,209 combined observations from the aforementioned satellites.

2.1 MODIS data

The MODIS, an advanced instrument aboard NASA's Terra and Aqua satellites, acquires data across 36 spectral bands, encompassing wavelengths from visible to thermal infrared (0.4 to 14.4 μm). Its passive sensors relies mostly on naturally available energy: Sun's energy reflected from the object or absorbed and reemitted (Ackerman et al., 1998). It provides data at various spatial resolutions—250 meters, 500 meters, and 1 kilometer with swath width of 2,330 kilometers which observes the entire Earth every one to two days. Cloud detection results are stored in the 48-bit "Cloud Mask" product, known as MYD35 for Aqua, while cloud properties can be found in MYD06 dataset. As an imager, MODIS provides column-integrated radiances, what limits the possibilities for cirrus retrieval.

For this research, we assessed the version of Collection 061 data, which is available in 5-minute granules at a spatial resolution of 1 km per pixel (at nadir). Each MYD35 and MYD06 file is paired with a MYD03 "Geolocation file" product that contains longitude and latitude information for each individual cloud mask IFOV (Instantaneous Field of View, Guenther et al. (2002).

2.1.1 The MODIS Cloud Mask product

The MODIS Cloud Mask product is a Level 2 dataset produced at spatial resolutions of 1-km and 250-m (at nadir). The cloud masking procedure is detailed in the works of Ackerman et al. (1998); Frey et al. (2008); Baum et al. (2012). The algorithm utilizes a sequence of visible and infrared threshold and consistency tests to determine the confidence level that an unobstructed view of the Earth's surface is achieved. The MYD35 dataset includes data from the Aqua satellite.

In this research, we considered 6 ready-to-use MODIS tests. Individual tests were described by Ackerman et al. (1998):

- Thin Cirrus test (SOLAR) – the solar channels in MODIS cover a range of wavelengths primarily in the visible and near-infrared spectrum (0.4 to 2.5 μm). This test uses the solar range to set the confident clear and middle thresholds to define the range of expected reflectances from thin cirrus. It indicates that a thin cirrus cloud is likely to be present. Test is only useful during daytime.

- Thin Cirrus test (IR) – the purpose of this test is detecting thin cirrus clouds. Channels used for this test are 11 μm an 12 μm (infrared (IR) range), incorporated to the split window technique.

- High Cloud Test (BT13.9) – applying CO2 absorption channels (around 14 μm) is a simple technique got from the CO2 slicing method (suitable for determining middle and upper troposphere ice clouds heights and effective amounts). This test is useful for high-level cloud detection, while it can reveal clouds above 500 hPa.

- High Cloud Test (BT6.7) – test designed for detecting thick high clouds. Starting from the ground level, the 6.7 μm radiation emitted by the surface or low clouds is absorbed in the atmosphere, therefore the signal is not received by an

https://doi.org/10.5194/amt-2024-163
Preprint. Discussion started: 1 October 2024


Atmospheric Measurement Techniques Discussions

instrument. The water vapor in layer in the atmosphere between 200 hPa and 500 hPa is the only source of the 6.7 μm radiation in clear-sky observation. Thick clouds placed above or near the 200 hPa level can be distinguish from clear sky or lower clouds.

- High Cloud Test (BT1.38) – the 1.38 μm channel lies in the strong water vapor absorption region. That results in obscuration of the most of Earth's surfaces, as well as attenuation of reflectance from low- and mid-level clouds. Pixels with this test applied, reveals high-level thin clouds as brighter. Unfortunately, the test has certain limitations, including its applicability to nighttime conditions, polar regions, midlatitude winters, and high elevations..
- High Cloud Test (BT3.9-12.0) – the 3.9-12.0 μm BTD (Brightness Temperatures Difference) test is specifically designed for nighttime observations over land and polar snow/ice surfaces. It is effective in distinguishing between thin cirrus clouds and cloud-free conditions and exhibits relative insensitivity to the atmospheric water vapor content (Hutchinson and Hardy, 1995).

Additionally, we independently developed unification of all tests, which we called All Tests Consolidation (ATC). If any one of the nine tests (t) detected cirrus clouds, we set the output flag (OF) to indicate cirrus.

If $\exists i \in \{1, 2, ..., 9\}$ $(t_i = 1)$ then ATCOF = 1.

Conversely, if no cirrus clouds were detected by all of the tests, provided they were all conducted, no cirrus flag was set.

If $\forall i \in \{1, 2, ..., 9\}$ $(t_i = 0)$ then ATCOF = 0.

ATC is essentially an adaptation of the MOD35 approach, but it is limited to tests that provide insights specifically about cirrus clouds.

2.1.2 The MODIS Cloud Product

As described by Menzel et al. (2015) the MODIS Cloud Product uses a combination of infrared and visible techniques to determine cloud physical and radiative properties. It derives cloud-particle phase, effective particle radius, and optical thickness from visible and near-infrared radiances, and indicates cloud shadows. Infrared methods provide cloud-top temperature, height, effective emissivity, phase, and cloud fraction, both day and night, at 1-km-pixel resolution. Additionally, the product includes cirrus reflectance at 1-km resolution to correct for cirrus scattering in land-surface reflectance. For Aqua satellite, dataset is called MYD06.

Beside ready-to-use MODIS tests (Section 2.2.1), other criteria may be applied using available for MODIS and CALIOP data, e.g. the ISCCP's (The International Satellite Cloud Climatology Project; https://isccp.giss.nasa.gov), which was established in 1982 as part of the World Climate Research Programme (WCRP; https://www.wcrp-climate.org/) to gather the global distribution of clouds, their properties, and their diurnal, seasonal, and interannual variations) definition of cloud types. The

https://doi.org/10.5194/amt-2024-163
Preprint. Discussion started: 1 October 2024

Atmospheric Measurement Techniques Discussions

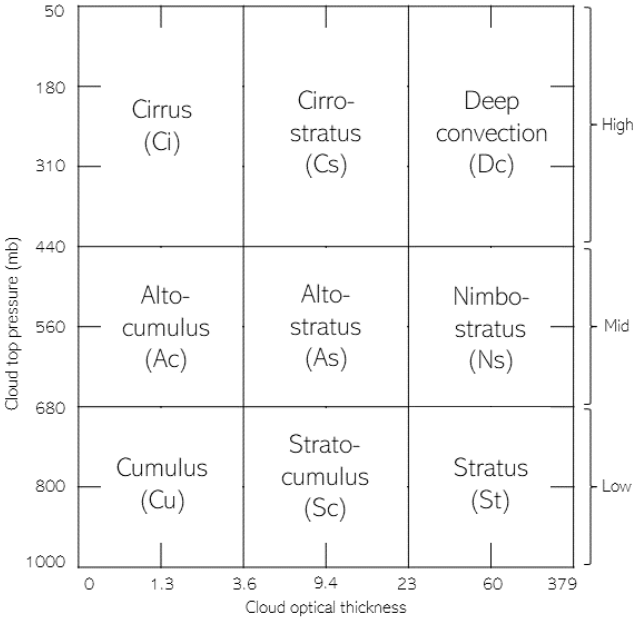

Figure 1. The distribution of cirrus clouds according to the evaluation.

developers of ISCCP deserve significant recognition for their foresight, as more than fourty years later, ISCCP continues to be a leading reference for describing the cloudy atmosphere. By examining visible and infrared radiances from geostationary and polar-orbiting meteorological satellites and making assumptions about cloud layering, thermodynamic phases, and properties, ISCCP characterizes a cloudy satellite pixel using the column visible optical depth (COT) and the cloud-top pressure (CTP) of the highest cloud layer. This information can be used to classify different cloud types as shown in the figure 1 (Rossow and Schiffer, 1991).

COT and CTP is also available for MODIS, within MYD06 standard product, and we used it to generate cirrus masks according to ISCCP definition. We considered two variants of the mask, defining cirrus as:

- a cloud with an optical thickness less than 3.6 and a top pressure below 440 hPa (hereinafter ISCCP3.6 test),
- a cloud with an optical thickness less than 23 and a top pressure below 440 hPa (hereinafter ISCCP23 test).

https://doi.org/10.5194/amt-2024-163
Preprint. Discussion started: 1 October 2024


Atmospheric Measurement Techniques Discussions

2.2 CALIOP data

Active sensors, in example CALIOP, operate day and night. Unlike passive methods, CALIOP's cloud detection accuracy is even higher at night than during the day (McGill et al., 2007). CALIOP provides high-resolution atmospheric profiles, with vertical resolutions ranging from 30 m below 8.2 km to 180 m above 20.1 km, and 60 m between these altitudes (M.Winker et al., 2006). This capability allows for clear distinction between cirrus and lower cloud layers, making CALIOP excellent for cirrus detection. Additionally, lidar can detect cirrus clouds with an optical depth of 0.01 or less (Vaughan et al., 2009), a capability beyond the reach of other imagers (Ackerman et al., 2008).

In this research, the lidar level-2 cloud layer at 5-km horizontal resolution, version 4.20 (CAL_LID_L2_05kmCLay-Standard-V4–20) product was used. As described by Liu et al. (2009) and Vaughan et al. (2009) this product reports cloud layers and cloud type information, with cirrus as a separate class. There are seven categories including clouds and aerosols. Inside the cloud class, 8 subtypes can be found (i.e. cirrus). Quality of CALIOP's detection is described by CAD (cloud-aerosol discrimination) score, which ranges from -100 to 100. Value -100 indicates high confidence of aerosol detection; value 100 shows that cloud was detected with high confidence; medium value (0) means that there is the same probability that the feature is cloud or aerosol (Liu et al., 2009; Vaughan et al., 2009). In this study, we only use observations with a CAD score higher than 80. The optical depth is also provided in this (CAL_LID_L2_05kmCLay-Standard-V4–20) CALIOP product.

For the purpose of this research, we regard CALIPSO as the reference for cirrus clouds detection. This choice is driven by the lidar's high sensitivity to optically thin clouds and its reliable performance in both daytime and nighttime conditions.

2.3 Matching datasets

NASA and its partners operate a group of Earth-observing satellites in sun-synchronous polar orbits, known as the Afternoon Constellation. This constellation has changed over time as satellites have moved out of the constellation or have deorbited, but Aqua remained a key member while CALIPSO began to move out of it in 2018. Afternoon Constellation crosses the equator in a northbound direction around 1:30 PM local solar time, providing near-simultaneous observations from multiple instruments. Aqua and CALIPSO, with nearly identical orbital configurations, operated in close proximity from 2006 to 2018, trailing by approximately one minute (Stephens et al., 2018), enabling synchronized observation times and a shared 16-day revisit cycle despite slightly differing ground tracks.

Using CALIOP data for the calibration and validation of atmospheric products from various space missions is a well-established practice. This method has been extensively applied to Aqua MODIS (Baum et al., 2012; Holz et al., 2009; Kotarba, 2020; Sun-Mack et al., 2014; Wang et al., 2016; Xie et al., 2010).

For this study, Aqua MODIS data and corresponding CALIOP observations for 2015 were matched. The matching process involved selecting a MODIS IFOV and comparing it with the corresponding CALIOP profile, ensuring the geometric center fell within the selected MODIS IFOV. Due to the orbital configuration of the two missions, CALIOP could only sample MODIS IFOVs near the MODIS nadir because of nadir-pointing instrument, preventing matching observations across the entire MODIS swath. Despite the length of the period (1 year), the procedure resulted in a sufficient number of observations (136,272,209

https://doi.org/10.5194/amt-2024-163
Preprint. Discussion started: 1 October 2024

Atmospheric Measurement Techniques Discussions

paired MODIS-CALIOP observations) as each MODIS granule contains approximately 2,030 IFOVs, and a full day of Aqua observations produces 288 granules. The aggregated MODIS–CALIOP statistics were compiled into global maps, each with a spatial resolution of 5° in both longitude and latitude.

2.4 Evaluation of MODIS data

The comparison was conducted at the pixel level, using a confusion matrix as the basis for calculations. It gives a detailed comparison of the model's predictions against the actual results. Structure of confusion matrix is presented in Tab. 1. and includes the following elements:

- True Positives (TP): The count of cases where MODIS accurately identified the existing (according to CALIOP) cirrus.
- False Positives (FP): The count of cases where MODIS incorrectly identified the high-level cloud, meaning it detected cirrus presence when it was actually absent.
- True Negatives (TN): The count of cases where MODIS correctly did not detect the presence of the cloud.
- False Negatives (FN): The count of cases where MODIS overlooked the cirrus occurrence.

Table 1. Confusion matrix

CALIPSO (reference data)	**Cirrus**	**No Cirrus**
MODIS Cirrus	True positive (TP)	False positive (FP)
MODIS No Cirrus	False negative (FN)	True negative (TN)

Every result undergoes a thorough validation through different parameters estimation using feature-based statistics (Stanski et al., 1989). To describe the data accuracy, probability of detection (POD) characteristics [1] and false alarm rate (FAR) statistic [2] were calculated: Probability of detection (POD) – is a metric used to assess the effectiveness of a detection system. In the context of cloud detection, POD indicates how well the detection algorithm correctly identifies the presence of clouds when they are actually present. A higher POD value signifies better performance of the detection system.

$$POD = TP/(TP + FN) \tag{1}$$

False alarm rate (FAR) – is a metric that measures the frequency of incorrect positive detections by a system. In the context of cloud detection, a lower FAR indicates a more accurate system, with fewer instances of falsely identifying clouds when they are not present.

$$FAR = FP/(FP + TN) \tag{2}$$

https://doi.org/10.5194/amt-2024-163
Preprint. Discussion started: 1 October 2024


Atmospheric Measurement Techniques Discussions

The incident frequencies within the matrix enabled the identification of two more diagnostic measures: Overall accuracy (OA) – is a metric that measures the proportion of correct predictions made by a detection system out of all predictions. In cloud detection, higher overall accuracy indicates that the system effectively identifies both the presence and absence of clouds correctly.

$$OA = (TP + TN)/n \tag{3}$$

Cohen's kappa k – Cohen's kappa is a statistical metric used to assess the degree of agreement between two raters or classification methods. Its scale ranges from -1 to 1, where a value of 1 represents perfect agreement, 0 indicates agreement no better than chance, and negative values indicate agreement worse than chance. In cloud detection, a higher kappa value indicates stronger agreement between the detected presence of clouds and their actual presence, while considering the possibility of random agreement.

$$k = (OA - PE)/(1 - PE) \tag{4}$$

where

$$PE = [(TP + FP)(TP + FN) + (TN + FP)(TN + FN)]/n^2 \tag{5}$$

$$n = TP + FP + FN + TN \tag{6}$$

The accuracy of high-level cloud detection was evaluated using the aforementioned metrics, differentiated by day and night, latitude, cloud optical depth, the number of detected cloud layers, and land classification. This assessment was conducted for the entire year 2015, as well as specifically for January and July (those two months are presented to exemplify the characteristics of two distinct seasons).

2.5 Bootstrap sampling

Due to the nature of cirrus cloud occurrences (18.7% in 2015, see Section 3), we can assume that the data sample will be imbalanced and one class (without cirrus) significantly outnumbers the other. Therefore, for such data, the appropriate statistical method to apply is bootstrap sampling (Efron, 1980). The balancing the sample stems from the issue of class imbalance, potentially skewing the statistical analysis and leading to biased results. To mitigate this, the bootstrap method is employed to artificially balance the dataset. This involves resampling the data with replacement, to ensure that each class has a comparable number of instances. By doing so, the analysis can yield more reliable, rather than being dominated by the majority class. When a sample is drawn from a population, the statistical measures derived from that exhibit sampling variability. The fundamental

https://doi.org/10.5194/amt-2024-163
Preprint. Discussion started: 1 October 2024


Atmospheric Measurement Techniques Discussions

concept of bootstrap revolves around resampling the original dataset with replacement to generate multiple bootstrap samples. In our study, for 1000 iterations, we selected a sample with replacement that included all observations indicating the presence of cirrus clouds (according to CALIPSO), as well as an equal number randomly drawn from the remaining observations. Each time, the previously described measures were calculated. After performing these calculations 1000 times, the average of these measures was computed.

The bootstrap has been already widely used among climatological studies. It has been employed to, among others, estimate confidence interval (Jolliffe, 2007), forecast storm track (Wilks et al., 2009), project future climate (Orlowsky et al., 2010), verify potential predictability of seasonal mean temperature and precipitation (Feng et al., 2011), study seasonal prediction of drought (Behrangi et al., 2015), inspect macrophysical properties of tropical cirrus clouds (Thorsen et al., 2013), evaluate sampling error in TRMM/PR rainfall products (Iida et al., 2010).

3 Cirrus clouds in 2015

Before conducting an analysis to assess the agreement in high-level cloud detection between CALIOP and MODIS data, we examined the cirrus coverage in 2015 according to reference data (CALIOP). The distribution of cirrus clouds (Fig. 2.) varies globally and is affected by factors such as latitude and atmospheric dynamics. Based on the CALIOP dataset, cirrus cloud coverage reached 18.7% in 2015, daytime coverage of high-level clouds in 2015 was recorded at 13.2% (Fig. 2a.), whereas nighttime coverage was higher, measured at 23.3% (Fig. 2b.). Near the equator, especially within the tropical belt, cirrus cloud cover exhibits peak values throughout the year, reaching approximately 35% during nighttime and 20% during daytime. In certain locations, particularly during nighttime, the high-level cloudiness has been observed to exceed 50%. In the mid-latitudes of both hemispheres, the distribution of clouds varies with the seasons, generally showing lower coverage compared to low latitudes, approximately 10% during daytime and 20% at night. In polar regions, particularly above approximately 60° latitude, cirrus cloud cover tends to be higher than in mid-latitudes, with nighttime coverage generally higher than daytime (Fig. 3.).

Additionally, CALIOP, measures the cloud optical thickness (COT) for individual layers as well as for the entire atmospheric column (Fig. 4.). When CALIOP detects multiple cirrus cloud layers, the COT values for all layers flagged as Cirrus are summed. The mean COT for cirrus clouds was 0.72 during daytime and 0.84 at nighttime. For the entire column (all cloud layers in column), the average COT measured by CALIOP was 4.26 during the day and 4.20 at night.

4 Evaluation of MODIS data

Using CALIPSO data as the reference, nine methods for detecting cirrus clouds with MODIS data were evaluated. All tests were applicable during daytime, whereas only five could be utilized at nighttime due to the requirement of solar illumination. Described in section 2 measures are presented in tab. 2. The parameters that, in our opinion, precluded the use of the test have been highlighted in bold. Additionally, they are preceded with the rate of observations performed (ROP) parameter, which is

https://doi.org/10.5194/amt-2024-163
Preprint. Discussion started: 1 October 2024

Atmospheric Measurement Techniques Discussions

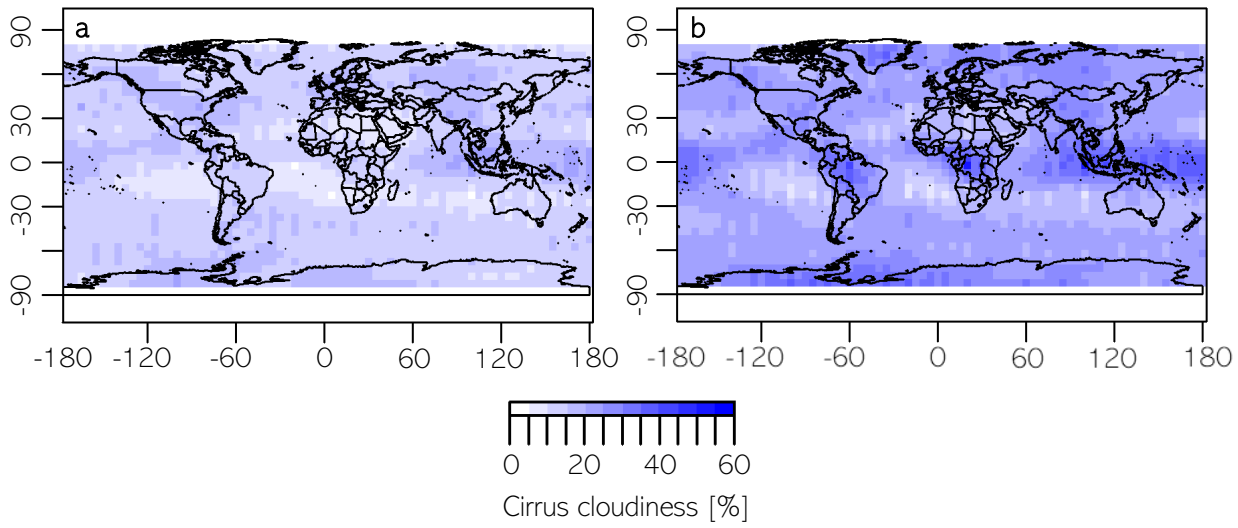

Figure 2. The distribution of cirrus clouds according to the evaluation.

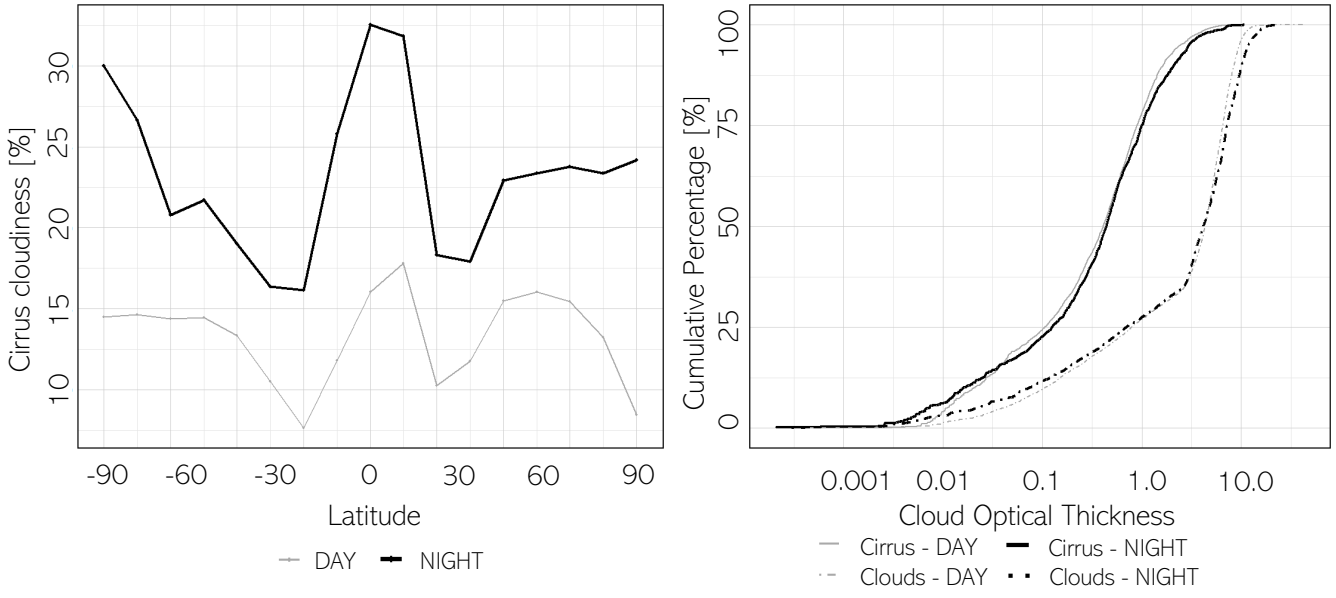

Figure 3. Cirrus coverage as a function of latitude (left) and Cumulative ratio of cirrus clouds with respect to COT (right)

https://doi.org/10.5194/amt-2024-163
Preprint. Discussion started: 1 October 2024

Atmospheric Measurement Techniques Discussions

the fraction of total observations for which the specific test could be conducted.

During daytime, the first four methods (SOLAR, IR, BT13.9, BT6.7) exhibited notably low detection effectiveness (with POD ranging between 0.33 and 15.79%), as well as low kappa coefficients (0.01-0.48). Although the test was performed on a relatively high proportion of observations (78.37% - 97.59%), with a low number of false alarms (FAR between 1.23% and 13.16%) and good overall accuracy (OA ranging between 48.61% and 53.80%), the poor detection capabilities (indicated by POD) rendered these data inadequate as reliable sources of information on the occurrence of Ci clouds. The differing parameters excluded tests BT3.9-12.0 and those with ISCCP criteria from consideration. The limited number of observations with available results from these tests rendered them impractical for use.

The two tests most effective globally were BT1.38 and ATC. With very similar parameters (POD, FAR, OA and Kappa)

Table 2. Goodness-of-fit of cloud detection between MODIS and CALIOP. Bold - parameters that precluded the use of the test

	Daytime					Nighttime				
Test	**ROP [%]**	**POD**	**FAR**	**OA**	**k**	**ROP [%]**	**POD**	**FAR**	**OA**	**k**
SOLAR	78.37	**15.79**	13.16	51.66	**0.03**	**0.00**	NA	NA	NA	NA
IR	83.32	**12.56**	4.37	53.80	0.48	73.98	**10.59**	3.27	54.94	0.52
BT13.9	65.52	**1.35**	3.59	48.61	-0.02	71.02	**2.13**	3.42	50.67	**-0.01**
BT6.7	97.59	**0.33**	1.23	49.92	**-0.01**	91.44	**0.60**	1.58	50.23	**-0.01**
BT1.38	78.37	77.76	28.28	74.71	0.49	**0.00**	NA	NA	NA	NA
BT3.9-12.0	**7.39**	64.48	15.36	72.41	0.46	**38.09**	39.09	5.46	65.26	0.33
ATC	98.67	80.87	34.86	72.98	0.46	94.84	25.46	6.90	59.50	0.19
ISCCP23	**37.97**	84.16	72.00	61.26	**0.13**	**0.00**	NA	NA	NA	NA
ISCCP3.6	**37.97**	33.30	16.54	58.96	**0.17**	**0.00**	NA	NA	NA	NA
January										
	Daytime					**Nighttime**				
Test	**ROP [%]**	**POD**	**FAR**	**OA**	**k**	**ROP [%]**	**POD**	**FAR**	**OA**	**k**
SOLAR	74.84	**15.08**	13.50	49.28	**0.02**	**0.00**	NA	NA	NA	NA
IR	78.95	**12.47**	4.54	51.81	0.46	72.30	**10.53**	3.46	54.07	0.51
BT13.9	67.59	**1.66**	3.66	46.28	**-0.02**	72.26	**2.36**	3.32	49.65	**-0.01**
BT6.7	97.95	**0.23**	1.09	49.68	**-0.01**	99.97	**0.59**	1.43	49.59	**-0.01**
BT1.38	74.84	79.65	31.69	74.22	0.48	**0.00**	NA	NA	NA	NA
BT3.9-12.0	**7.02**	56.89	13.50	69.48	0.41	**41.19**	35.00	3.80	64.37	0.30
ATC	98.98	80.23	34.17	73.03	0.46	99.98	23.38	6.12	58.63	99.98
ISCCP23	**38.55**	84.27	68.88	64.10	**0.17**	**0.00**	NA	NA	NA	NA
ISCCP3.6	**38.55**	33.38	14.58	59.27	**0.19**	**0.00**	NA	NA	NA	NA
June										
	Daytime					**Nighttime**				
Test	**ROP [%]**	**POD**	**FAR**	**OA**	**k**	**ROP [%]**	**POD**	**FAR**	**OA**	**k**
SOLAR	84.32	**16.57**	11.58	53.99	**0.05**	**0.00**	NA	NA	NA	NA
IR	92.26	**11.99**	3.76	54.17	0.49	68.77	**10.02**	2.61	57.81	0.56
BT13.9	65.65	**1.89**	3.72	49.61	**-0.02**	67.48	**2.62**	3.93	53.88	**-0.01**
BT6.7	99.69	**0.15**	1.06	49.63	**-0.01**	81.30	**0.84**	1.96	52.06	**-0.01**
BT1.38	84.32	74.97	22.06	76.52	0.53	**0.00**	NA	NA	NA	NA
BT3.9-12.0	**7.67**	72.20	21.54	74.30	0.47	**37.58**	47.02	7.95	67.82	0.38
ATC	99.96	83.14	31.76	75.69	0.51	88.61	30.47	7.99	62.05	0.23
ISCCP23	**36.57**	85.54	74.77	61.16	**0.12**	**0.00**	NA	NA	NA	NA
ISCCP3.6	**36.57**	32.84	16.26	58.67	**0.17**	**0.00**	NA	NA	NA	NA

https://doi.org/10.5194/amt-2024-163
Preprint. Discussion started: 1 October 2024


Atmospheric Measurement Techniques Discussions

the ATC test demonstrated superiority due to a significantly higher number of available observations (78.37% vs 98.67%, respectively).

Among the night tests, IR, BT13.9, and B6.7 exhibited low detection capabilities (POD 0.60% - 10.59%), whereas the BT3.9-12.0 test was performed only on 38.09% of observations. As with the daytime tests, the ATC test proved to be the most suitable for detection. Considering that global statistics for January and July were not markedly different from the yearly averages (Tab. 2.), subsequent analyses were conducted using data from the entire year.

As previously mentioned, all statistical measures were also calculated for different latitudes (Fig. 4.). The observed latitudinal variability can be attributed to the physical properties of the respective radiation range and the intended function of the specific channel, as well as to the spatial distribution of cirrus clouds occurrence. For almost all of tests we observe the ROP (Fig. 4a. & Fig. 4b.) decrease with the latitude increase. This is related to presence of solar illumination. The exception is ROP according to BT3.9-12.0 (increase from 0% in tropics to almost 30% in polar region) which was specifically designed for nighttime observations over land and polar snow/ice surfaces. ROP for both tests using ISCCP criteria is equal.

The latitudinal distribution of POD during the day (Fig. 4c.) shown that ISCCP criteria the most accurately detected cirrus clouds in the tropical regions (up to 75% for ISCCP23 and almost 100% for ISCCP3.6), with POD reduction with latitude decrease (to about 10% and 40% respectively). Similar pattern was observed i.e. for BT13.9 method, but with cirrus detection capabilities about 3 times inferior. Depending on the test, latitudinal variability of POD could be also higher for mid-latitudes (ATC), low latitudes (test utilizing the solar radiation range), or remained relatively unchanged. There is no clear trend of increasing/decreasing POD with latitude during the night (Fig. 4d.; slightly more cirrus correctly detected for polar regions by IR, BT13.9 and BT3.9-12.0 tests). The mid-latitudes exhibit POD drop for BT6.7 test, and consequently ATC test.

Figure 5 (Fig. 4e. & Fig. 4f.) shows also the latitudinal variability of FAR. In the tropical regions most of the tests show peak of falsely reported cirrus clouds during daytime in equatorial region (with maximum exceeding 90% for ISCCP23 and 50% for ISCCP3.6). Additionally, BT1.38 test falsely detects cirrus more often with latitude increase, what results with 'bimodal' FAR distribution with peaks in tropics (about 35%) and midlatitudes (75% for northern hemisphere and 30% for southern). A distribution resembling BT1.38 exhibited test ATC, but with an upward shift of about 10 percentage points. Relatively few falsely observed cloud cases, with similar to the daytime distribution, were detected at night. No significant differences were found between the equatorial and polar regions for all the tests for OA. For the daytime the latitudinal variation was more readily observable and varied (Fig. 4g. & 4i. vs Fig. 4h. & 4j.).

Considering the very high proportion of correctly detected cirrus clouds, the high overall accuracy and kappa coefficient (degree of agreement between two classification methods), ATC test showed the highest agreement with CALIOP data. Additionally, it covers nearly all observations in the test (96.7%) and shows relatively low variability of statistical measures across different latitudes. Therefore can be used as a basis for study evaluating cirrus cloud coverage in long term perspective.

To ensure ATC test performs optimally under various conditions and to provide a comprehensive analysis, fit measures were additionally evaluated for "number of layers found" (NLF, Fig. 5.) and IGBP (The International Geosphere–Biosphere Programme, tab. 4).

Since CALIOP is a lidar providing high-resolution atmospheric profiles, with vertical resolutions ranging from 30 m to 180

https://doi.org/10.5194/amt-2024-163
Preprint. Discussion started: 1 October 2024

Atmospheric Measurement Techniques Discussions

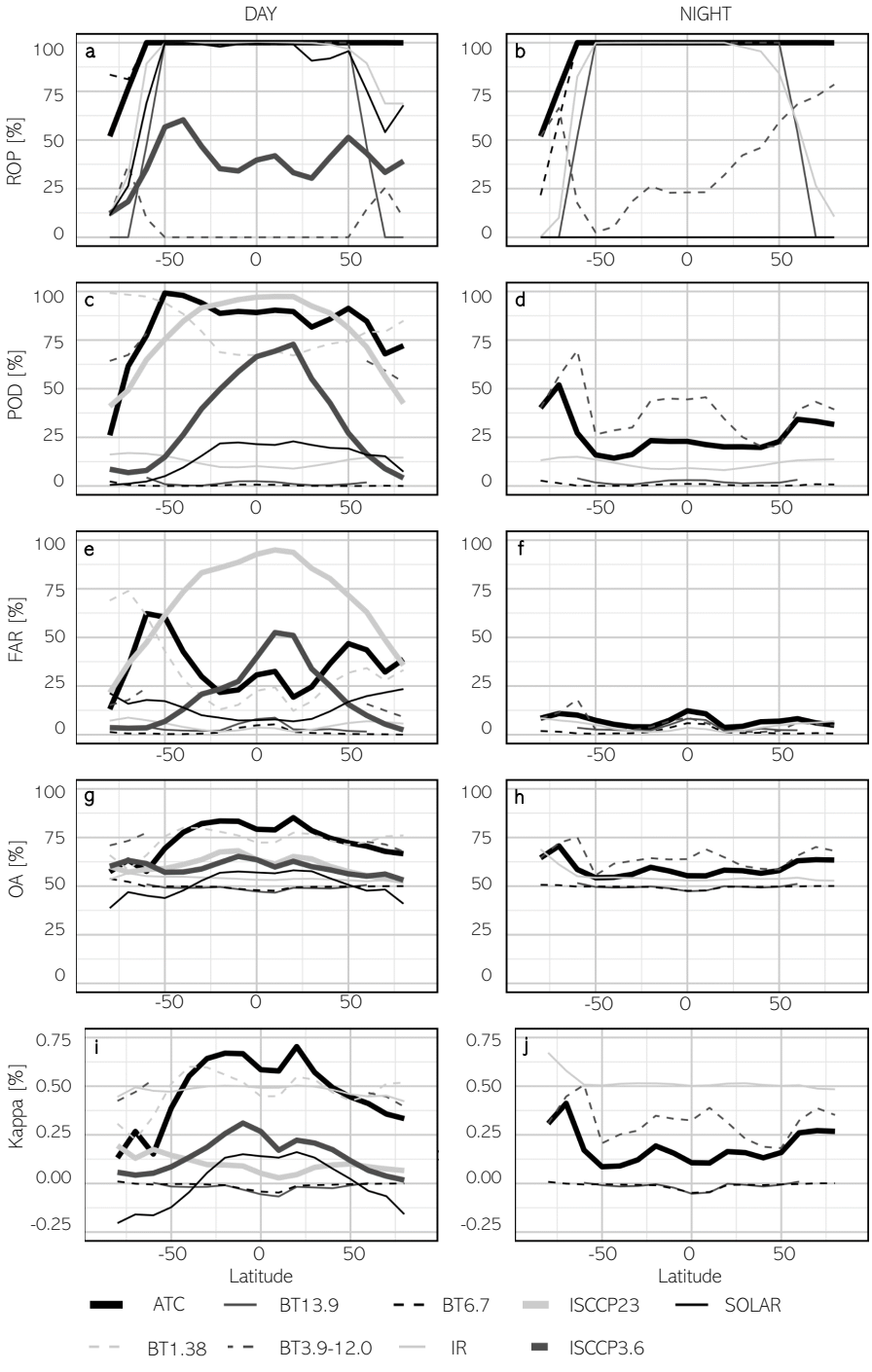

Figure 4. Cirrus detection accuracy with respect to the latitude (letters (a, . . . , j) used to facilitate reference in the text)

https://doi.org/10.5194/amt-2024-163
Preprint. Discussion started: 1 October 2024


Atmospheric Measurement Techniques Discussions

m, it's output could be divided into maximum 10 cloud layers. When multiple cloud layers overlap, the lidar signal may be attenuated, potentially leading to underestimation of cloud detection. Our research evaluated the collocation of MODIS data to the reference CALIOP data, segmented by the number of detected cloud layers excluding cirrus clouds. A zero indicated that no other cloud layers were detected besides possible cirrus in a given profile. Both day and night observations revealed a maximum of four additional cloud layers. Based on the test conducted, ROP either decreased (i.e. BT13.9 70% to 30% at daytime or BT3.9-12.0 at nighttime), increased (7% to 25% at daytime for BT3.9-12.0), or remained stable with an increasing number of cloud layers (Fig. 5a. & Fig. 5b.). For ATC test, no discernible trend was identified. No clear trend could be observed for POD, both day and night (Fig. 5c. & Fig. 5d.). However, the distribution of FAR parameter exhibited a different pattern. In multiple tests, notably ATC test, the value of FAR (Fig. 5e. & Fig. 5f.) significantly elevated with an increasing number of cloud layers (9% to 78% during day and 1% to 15% at night for ATC). Presumably, for clouds with significant vertical development (with more detected layers), MODIS identified only the uppermost layer, incorrectly categorizing it as the complete cloud profile. Increasing number of falsely reported cirrus with NLF manifests itself in OA and Kappa distribution. With the increase in non-cirrus layers found, there is a corresponding decrease in OA and Kappa, both for day and night (Fig. 5g., Fig. 5h., Fig. 5i. & Fig. 5j.).

The International Geosphere–Biosphere Programme (IGBP) defines ecosystems surface classifications. For purpose of this study, 17 IGBP groups was aggregated to 3 classes: water, land and snow (goodness-of-fit with respect to land classification is presented in tab. 4.). Bright surfaces like snow, ice deserts, or complex terrain with varying surface types can make it challenging to distinguish clouds from the ground. The first noticeable aspect is the significantly lower ROP for snow compared to other classes. Generally, the fit measures are similar to those in previous analyses. During the day, ATC test performs better over water, whereas SOLAR test performs better over land. On the contrary, during nighttime, BT3.9-12.0 test performs better over water, whereas ATC test performs better over land.

The analysis with respect to NLF and land cover types confirmed that ATC test is the most suitable for achieving the objective of this study. Therefore, the spatial distribution of the individual fit measures for this test was examined (Fig. 6).
Spatial distribution indicates very high level of ROP for both: day (Fig. 6a.) and night (Fig. 6b.) for the entire Earth. The southernmost regions of the Southern Hemisphere are an exception, exhibiting lower values. Spatial variations observed in correctly detected cirrus highlight differences between daytime and nighttime POD distribution (Fig. 6c. & Fig. 6d.). During the daytime, high values are observed over nearly the entire Earth's surface, with exceptions in the regions of Antarctica, Greenland and the Himalayas ($\geq$ 80% vs $\leq$ 20% respectively), which are regions covered with snow and ice. However, at night, the highest difference is between land and water ($\geq$ 50% vs c.a. 20%). Similar patterns to the POD distribution for day and night can be observed when considering OA (Fig. 6g. - Fig. 6h.). On both sides of the equator, FAR reaches the lowest values, being slightly higher during the day than at night (about 20% and $\leq$ 5%) and increasing with latitude, however, there is a reduction observed in regions covered by snow and ice (Fig. 6e. & Fig. 6f.). In regions with the highest rate of correctly detected and the lowest ratio of falsely reported cirrus general accuracy of classification (OA) exceeded 80% at daytime and an 50% at night. As well as OA, Kappa was higher during the day. During the day, Kappa values ranged from 0.5 to 1.0 for

https://doi.org/10.5194/amt-2024-163
Preprint. Discussion started: 1 October 2024

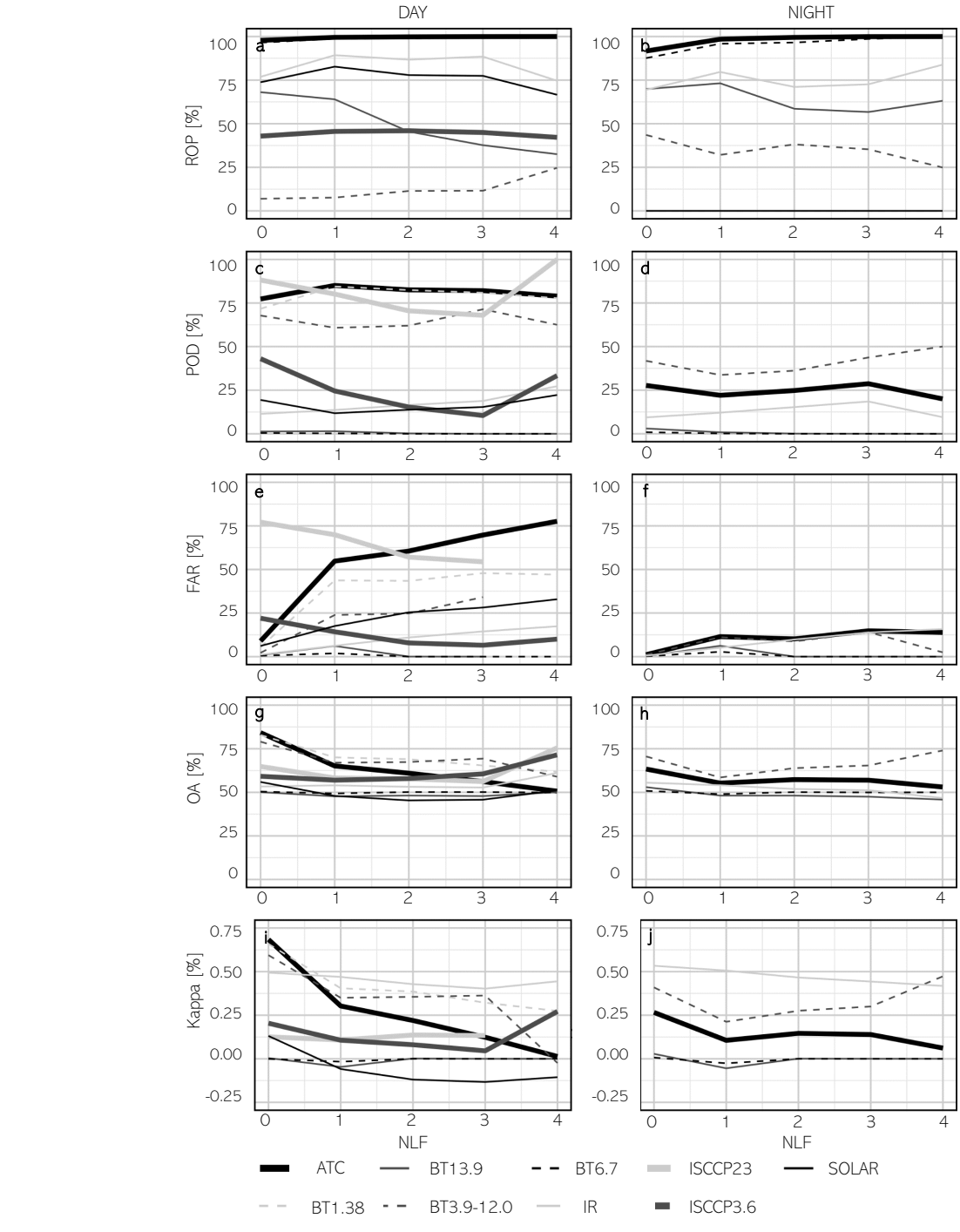

Figure 5. Cirrus detection accuracy with respect to the NLF (letters (a, . . . , j) used to facilitate reference in the text)

https://doi.org/10.5194/amt-2024-163
Preprint. Discussion started: 1 October 2024

Atmospheric Measurement Techniques Discussions

Table 3. Goodness-of-fit of cloud detection between MODIS and CALIOP with respect to land classification

WATER										
	Daytime					**Nighttime**				
Test	**ROP [%]**	**POD**	**FAR**	**OA**	**k**	**ROP [%]**	**POD**	**FAR**	**OA**	**k**
SOLAR	88.95	11.40	13.05	49.55	-0.02	0.00	NA	NA	NA	NA
IR	92.44	12.93	4.24	54.23	0.48	85.56	11.10	3.36	54.35	0.51
BT13.9	74.18	1.32	3.66	48.21	-0.02	79.41	1.98	3.37	49.90	-0.01
BT6.7	99.99	0.20	1.25	49.48	-0.01	99.98	0.52	1.57	49.48	-0.01
BT1.38	88.95	84.91	30.78	76.99	0.54	0.00	NA	NA	NA	NA
BT3.9-12.0	5.45	67.67	16.17	74.23	0.49	14.64	51.57	8.69	70.13	0.42
ATC	100.00	90.10	40.63	74.73	0.49	99.99	18.94	6.62	56.16	0.12
ISCCP23	29.32	86.27	73.48	62.45	0.14	0.00	NA	NA	NA	NA
ISCCP3.6	29.32	34.69	16.22	59.89	0.19	0.00	NA	NA	NA	NA
LAND										
	Daytime					**Nighttime**				
Test	**ROP [%]**	**POD**	**FAR**	**OA**	**k**	**ROP [%]**	**POD**	**FAR**	**OA**	**k**
SOLAR	84.11	27.39	12.70	57.53	0.15	0.00	NA	NA	NA	NA
IR	93.02	11.42	4.47	52.87	0.48	80.87	9.16	2.92	53.14	0.51
BT13.9	77.48	1.41	3.40	49.65	-0.02	86.30	2.49	3.58	49.46	-0.01
BT6.7	100.00	0.22	1.32	49.45	-0.01	100.00	0.49	1.64	49.42	-0.01
BT1.38	88.95	84.91	30.78	76.99	0.54	0.00	NA	NA	NA	NA
BT3.9-12.0	8.09	62.80	14.99	71.91	0.45	97.78	33.85	3.61	65.15	0.30
ATC	100.00	79.62	29.87	74.88	0.50	100.00	39.34	7.80	65.77	0.32
ISCCP23	45.98	83.88	76.09	58.95	0.08	0.00	NA	NA	NA	NA
ISCCP3.6	45.98	35.73	22.99	55.46	0.12	0.00	NA	NA	NA	NA
SNOW										
	Daytime					**Nighttime**				
Test	**ROP [%]**	**POD**	**FAR**	**OA**	**k**	**ROP [%]**	**POD**	**FAR**	**OA**	**k**
SOLAR	10.35	6.01	20.12	41.56	-0.14	0.00	NA	NA	NA	NA
IR	13.98	15.12	7.27	50.73	0.43	1.12	13.76	5.52	56.13	0.52
BT13.9	0.16	0.72	5.12	47.19	-0.04	0.16	2.59	5.06	49.70	-0.03
BT6.7	78.83	1.70	1.04	54.07	0.01	27.05	2.48	1.86	49.83	0.01
BT1.38	10.35	90.90	53.45	69.55	0.38	0.00	NA	NA	NA	NA
BT3.9-12.0	13.95	61.99	15.30	69.73	0.41	47.02	39.67	7.85	65.31	0.31
ATC	88.29	27.48	10.83	59.27	0.17	55.73	33.67	7.17	62.25	0.26
ISCCP23	11.34	46.54	31.07	57.85	0.16	0.00	NA	NA	NA	NA
ISCCP3.6	11.34	8.00	3.64	59.62	0.05	0.00	NA	NA	NA	NA

regions at low latitudes. In mid and high latitudes, Kappa values were between 0.0 and 0.5, remaining positive (Fig. 6i.). At night (Fig. 6j.), nearly the entire Earth's surface exhibited Kappa values between 0.0 and 0.5, with a negative Kappa observed in the vicinity of Micronesia.

5 Discussion and summary

This study aims to address the research gap by evaluating whether MODIS ready-to-use cloud mask product can be used for producing a cirrus mask. We also seek to identify the conditions under which this approach would be effective and when it

https://doi.org/10.5194/amt-2024-163
Preprint. Discussion started: 1 October 2024

Atmospheric Measurement Techniques Discussions

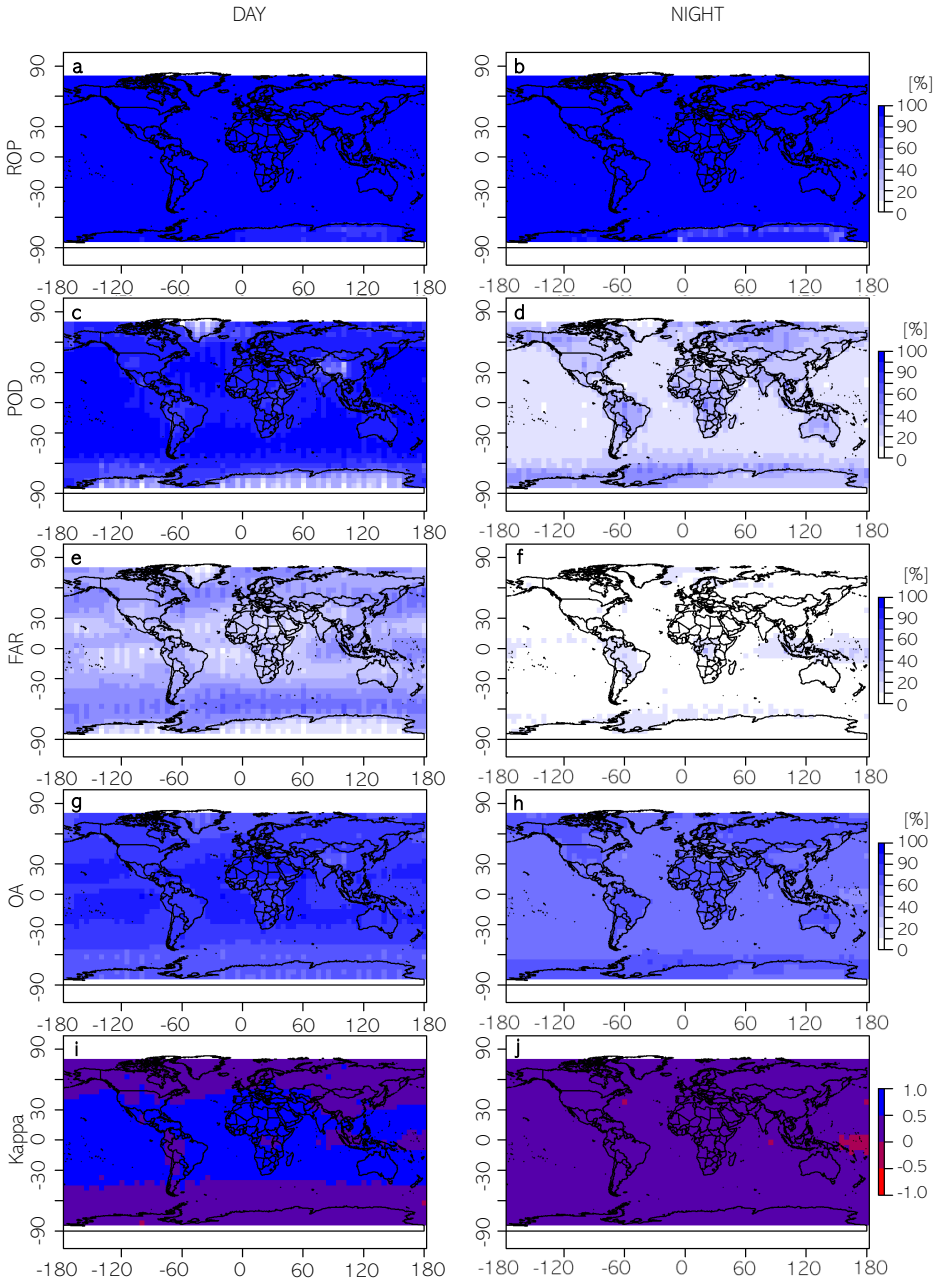

Figure 6. Spatial distribution of the accuracy detection of cirrus using ATC test (letters (a, . . . , j) used to facilitate reference in the text)

might not be suitable. The study found that it was possible however, certain limitations, particularly those related to nighttime, must be consistently considered.

https://doi.org/10.5194/amt-2024-163
Preprint. Discussion started: 1 October 2024


Atmospheric Measurement Techniques Discussions

During daytime, the two most effective tests were BT1.38 and ATC. With very similar parameters (POD, FAR, OA and Kappa) the ATC test demonstrated superiority due to a significantly higher number of available observations. Among the nighttime tests the ATC test proved to be the most suitable for detection. Additionally, ATC test covers nearly all observations in the test (96.7%) and shows relatively low variability of statistical measures across different latitudes. Spatial analysis indicates very high level of ROP for both: day and night for the entire Earth. Spatial variations observed in correctly detected cirrus highlight differences between daytime and nighttime POD distribution. During the daytime, high values are observed over nearly the entire Earth's surface, with exceptions in the polar regions and Himalayas. However, at night, land regions display higher POD values compared to the surrounding areas. Considering all mentioned above ATC test is proved to be the best among the available methods for detecting high-level clouds. However, it is evident that its utility during nighttime is significantly limited compared to daytime. Consequently, we have determined that it may be suitable for creating a high-level clouds mask and conducting a long-term climatological analysis of cirrus cloud coverage. This approach simultaneously allows us to address the second research gap mentioned in this paragraph, which concerns our lack of knowledge regarding the long-term variability of high-level cloud coverage.

Obtained from CALIOP data cirrus mask mentioned in Section 3 allow us to investigate the distribution of cirrus clouds (Fig. 2.) in 2015. Based on the CALIOP dataset, cirrus cloud coverage reached 18.7% in 2015, daytime coverage of high-level clouds in 2015 was recorded at 13.2%, whereas nighttime coverage was higher, measured at 23.3%.

In a similar manner, a cirrus mask was generated based on the MODIS data using ATC test. Derived from this data cirrus coverage (Fig. 7a.) daytime coverage of high-level clouds was recorded at 41.0%, whereas nighttime coverage was lower, measured at 10.9% (Fig. 7b.). Regrettably, this indicates that although achieving comparable outcomes as reported in existing literature (Sassen et al., 2008), the data concerning the diurnal pattern of cloud coverage is entirely lost.

We also compared cirrus cloud coverage in 2015 obtained from CALIOP and MODIS data (Fig. 8.). Mean difference between Cirrus coverage derived from CALIOP and MODIS was -27.71 p.p. for the daytime observations (Fig. 8a.), MODIS generally indicated higher cloud cover compared to CALIOP. On the contrary, mean difference between Cirrus coverage derived from CALIOP and MODIS was -12.31 p.p. for the nighttime observations (Fig. 8b.). While the relationship between MODIS and CALIOP is statistically significant ($p < 0.001$), the R^2 value of 0.165 indicates that MODIS captures only 16.5% of the variability. In the nighttime dataset, the R^2 improves to 0.422, meaning MODIS cloud coverage aligns better with CALIOP at night. Although the majority of fit metrics show improved performance during the day, the high number of false alarms ultimately results in the nighttime fit being more accurate when cirrus coverage is examined in the subsequent analysis.

In conclusion, our study has shown that ATC test, developed based on MODIS Cloud Product data, demonstrated the highest agreement with reference data (the overall accuracy of 72.98% during daytime and 59.50% at night, probability of detection: 80.87% and 25.46%, false alarm rate of 34.86% and 6.90%, and Cohen's kappa coefficient of 0.46 and 0.19 respectively). Although the study had certain limitations, such as nighttime cirrus detections, its results may have important implications for understanding the nature of high-level cloudiness. Future research may focus on long-term trends in cirrus cloudiness. These conclusions represent an important step toward a better understanding of the impact of clouds on the climate.

https://doi.org/10.5194/amt-2024-163
Preprint. Discussion started: 1 October 2024

Atmospheric Measurement Techniques Discussions

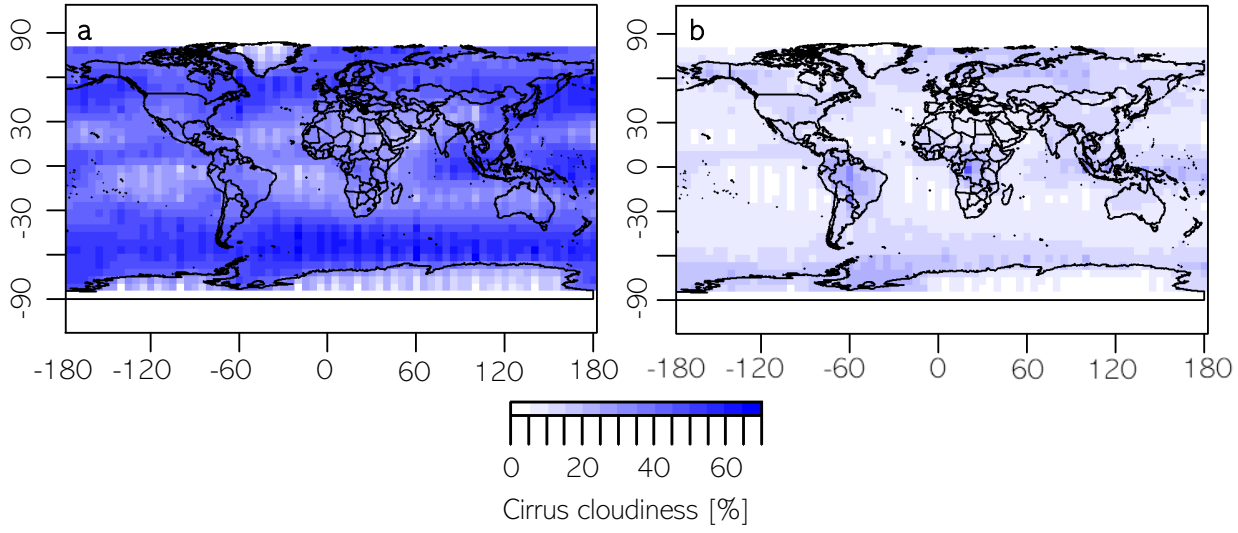

Figure 7. MODIS-based cirrus cloud coverage in 2015- daytime (a) and nighttime (b)

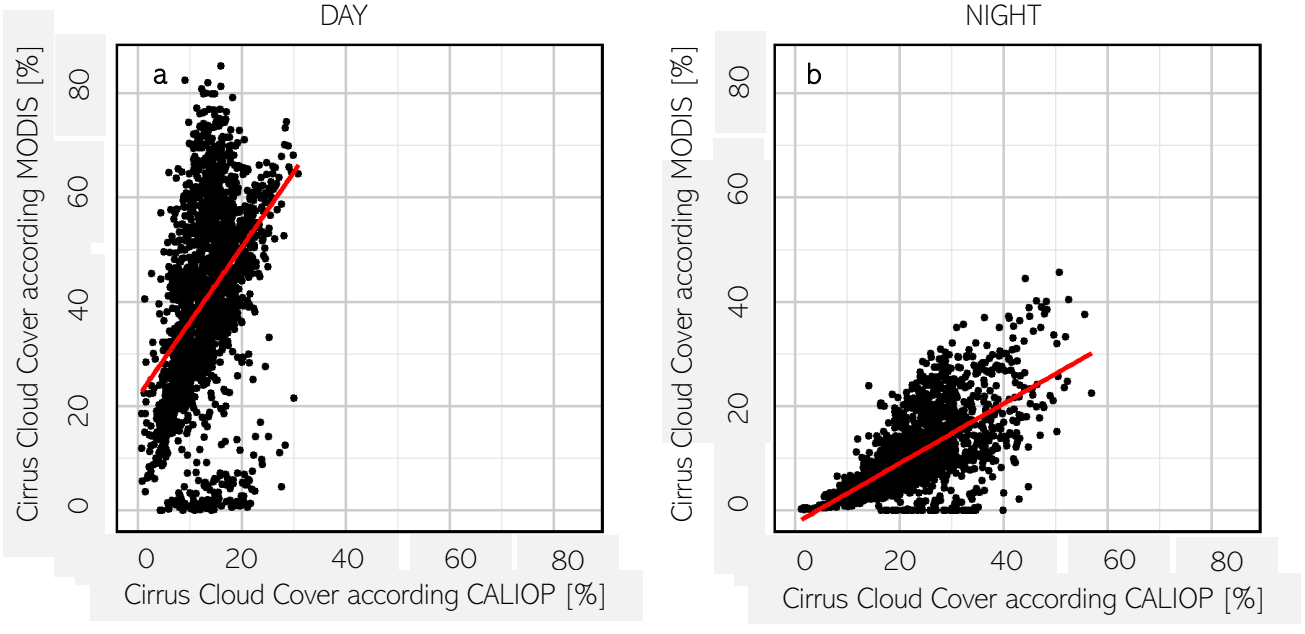

Figure 8. CALIOP-MODIS cirrus cloud coverage comparison in 2015- daytime (a) and nighttime (b)

https://doi.org/10.5194/amt-2024-163
Preprint. Discussion started: 1 October 2024

Atmospheric Measurement Techniques Discussions

Author contributions. Żaneta Nguyen Huu: conceptualization, data curation, formal analysis, funding acquisition, investigation, methodology, project administration, software, validation, visualization, writing – original draft preparation & editing

Andrzej Z. Kotarba: conceptualization, data curation, methodology, validation, writing – review & editing

Agnieszka Wypych: conceptualization, validation, writing – review & editing

Competing interests. The authors declare that they have no conflict of interest.

6 Acknowledgements

This work was supported by the National Science Center of Poland [grant number 2021/41/N/ST10/02274]. We gratefully acknowledge Poland's high-performance Infrastructure PLGrid ACK Cyfronet AGH for providing computer facilities and support within computational grant no PLG/2024/016949.

https://doi.org/10.5194/amt-2024-163
Preprint. Discussion started: 1 October 2024

Atmospheric Measurement Techniques Discussions

References

Ackerman, S. A., Liou, K.-N., Valero, F. P. J., and Pfister, L.: Heating Rates in Tropical Anvils, Journal of Atmospheric Sciences, 45, 1606–1623, 1988.

Ackerman, S. A., Strabala, K. I., Menzel, W. P., Frey, R. A., Moeller, C. C., and Gumley, L. E.: Discriminating clear sky from clouds with MODIS, Journal of Geophysical Research Atmospheres, 103, 32 141–32 157, https://doi.org/10.1029/1998JD200032, 1998.

Ackerman, S. A., Holz, R. E., Frey, R., Eloranta, E. W., Maddux, B. C., and McGill, M.: Cloud detection with MODIS. Part II: Validation, Journal of Atmospheric and Oceanic Technology, 25, 1073–1086, https://doi.org/10.1175/2007JTECHA1053.1, 2008.

Amato, U., Antoniadis, A., Cuomo, V., Cutillo, L., Franzese, M., Murino, L., and Serio, C.: Statistical cloud detection from SEVIRI multispectral images, Remote Sensing of Environment, 112, 750–766, https://doi.org/10.1016/j.rse.2007.06.004, 2008.

Baum, B. A., Menzel, W. P., Frey, R. A., Tobin, D. C., Holz, R. E., Ackerman, S. A., Heidinger, A. K., and Yang, P.: MODIS cloud-top property refinements for collection 6, Journal of Applied Meteorology and Climatology, 51, 1145–1163, https://doi.org/10.1175/JAMC-D-11-0203.1, 2012.

Behrangi, A., Nguyen, H., and Granger, S.: Probabilistic seasonal prediction of meteorological drought using the bootstrap and multivariate information, Journal of Applied Meteorology and Climatology, 54, 1510–1522, https://doi.org/10.1175/JAMC-D-14-0162.1, 2015.

Bock, L. and Burkhardt, U.: Reassessing properties and radiative forcing of contrail cirrus using a climate model, Journal of Geophysical Research, 121, 9717–9736, https://doi.org/10.1002/2016JD025112, 2016.

Campbell, J. R., Lolli, S., Lewis, J. R., Gu, Y., and Welton, E. J.: Daytime cirrus cloud top-of-the-atmosphere radiative forcing properties at a midlatitude site and their global consequences, Journal of Applied Meteorology and Climatology, 55, 1667–1679, https://doi.org/10.1175/JAMC-D-15-0217.1, 2016.

Chen, P. Y., Srinivasan, R., Fedosejevs, G., and Narasimhan, B.: An automated cloud detection method for daily NOAA-14 AVHRR data for Texas, USA, International Journal of Remote Sensing, 23, 2939–2950, https://doi.org/10.1080/01431160110075631, 2002.

Efron, B.: The Jackknife, the bootstrap, and other resampling plans, Tech. rep., 1980.

Eleftheratos, K., Zerefos, C. S., Zanis, P., Balis, D. S., Tselioudis, G., Gierens, K., and Sausen, R.: A study on natural and manmade global interannual fluctuations of cirrus cloud cover for the period 1984-2004, Atmospheric Chemistry and Physics, 7, 2631–2642, https://doi.org/10.5194/acp-7-2631-2007, 2007.

Feng, X., Delsole, T., and Houser, P.: Bootstrap estimated seasonal potential predictability of global temperature and precipitation, Geophysical Research Letters, 38, 1–6, https://doi.org/10.1029/2010GL046511, 2011.

Frey, R. A., Ackerman, S. A., Liu, Y., Strabala, K. I., Zhang, H., Key, J. R., and Wang, X.: Cloud detection with MODIS. Part I: Improvements in the MODIS cloud mask for Collection 5, Journal of Atmospheric and Oceanic Technology, 25, 1057–1072, https://doi.org/10.1175/2008JTECHA1052.1, 2008.

Frey, R. A., Ackerman, S. A., Holz, R. E., Dutcher, S., and Griffith, Z.: The continuity MODIS-VIIRS cloud mask, Remote Sensing, 12, 1–18, https://doi.org/10.3390/rs12203334, 2020.

Gu, L., Ren, R., and Zhang, S.: Automatic cloud detection and removal algorithm for MODIS remote sensing imagery, Journal of Software, 6, 1289–1296, https://doi.org/10.4304/jsw.6.7.1289-1296, 2011.

Guenther, B., Xiong, X., Salomonson, V. V., Barnes, W., and Young, J.: On-orbit performance of the Earth Observing System Moderate Resolution Imaging Spectroradiometer; first year of data, Remote Sensing of Environment, 83, 16–30, 2002.

https://doi.org/10.5194/amt-2024-163
Preprint. Discussion started: 1 October 2024

Heidinger, A. K. and Pavolonis, M. J.: Gazing at cirrus clouds for 25 years through a split window. Part I: Methodology, Journal of Applied Meteorology and Climatology, 48, 1100–1116, https://doi.org/10.1175/2008JAMC1882.1, 2009.

Holz, R. E., Ackerman, S. A., Nagle, F. W., Frey, R., Dutcher, S., Kuehn, R. E., Vaughan, M. A., and Baum, B.: Global Moderate Resolution Imaging Spectroradiometer (MODIS) cloud detection and height evaluation using CALIOP, Journal of Geophysical Research Atmospheres, 114, 1–17, https://doi.org/10.1029/2008JD009837, 2009.

Iida, Y., Kubota, T., Iguchi, T., and Oki, R.: Evaluating sampling error in TRMM/PR rainfall products by the bootstrap method: Estimation of the sampling error and its application to a trend analysis, Journal of Geophysical Research Atmospheres, 115, 1–14, https://doi.org/10.1029/2010JD014257, 2010.

Jolliffe, I. T.: Uncertainty and inference for verification measures, Weather and Forecasting, 22, 637–650, https://doi.org/10.1175/WAF989.1, 2007.

Kärcher, B.: Formation and radiative forcing of contrail cirrus, Nature Communications, 9, 1–17, https://doi.org/10.1038/s41467-018-04068-0, 2018.

Kinne, S. and Liou, K.-N.: The Effects of the Nonsphericity and Size Distribution of Ice Crystals on the Radiative Properties of Cirrus Clouds, Atmospheric Research, 24, 273–284, 1989.

Kotarba, A. Z.: Regional high-resolution cloud climatology based on MODIS cloud detection data, International Journal of Climatology, 36, 3105–3115, https://doi.org/10.1002/joc.4539, 2016.

Kotarba, A. Z.: Calibration of global MODIS cloud amount using CALIOP cloud profiles, Atmospheric Measurement Techniques, 13, 4995–5012, https://doi.org/10.5194/amt-13-4995-2020, 2020.

Kotarba, A. Z. and Nguyen Huu, Ż.: Accuracy of Cirrus Detection by Surface-Based Human Observers, Journal of Climate, 35, 3227–3241, https://doi.org/10.1175/JCLI-D-21-0430.1, 2022.

Li, Q. and Groß, S.: Satellite observations of seasonality and long-term trends in cirrus cloud properties over Europe : investigation of possible aviation impacts, Atmospheric Chemistry and Physics, 22, 15 963–15 980, 2022.

Liu, Y., Key, J. R., Frey, R. A., Ackerman, S. A., and Menzel, W. P.: Nighttime polar cloud detection with MODIS, Remote Sensing of Environment, 92, 181–194, https://doi.org/10.1016/j.rse.2004.06.004, 2004.

Liu, Z., Vaughan, M., Winker, D., Kittaka, C., Getzewich, B., Kuehn, R., Omar, A., Powell, K., Trepte, C., and Hostetler, C.: The CALIPSO lidar cloud and aerosol discrimination: Version 2 algorithm and initial assessment of performance, Journal of Atmospheric and Oceanic Technology, 26, 1198–1213, https://doi.org/10.1175/2009JTECHA1229.1, 2009.

Lolli, S., Campbell, J. R., Lewis, J. R., Gu, Y., Marquis, J. W., Chew, B. N., Liew, S. C., Salinas, S. V., and Welton, E. J.: Daytime top-of-the-atmosphere cirrus cloud radiative forcing properties at Singapore, Journal of Applied Meteorology and Climatology, 56, 1249–1257, https://doi.org/10.1175/JAMC-D-16-0262.1, 2017.

Macke, A., Francis, P. N., Mcfarquhar, G. M., and Kinne, S.: The role of ice particle shapes and size distributions in the single scattering properties of cirrus clouds, Journal of the Atmospheric Sciences, 55, 2874–2883, https://doi.org/10.1175/1520-0469(1998)055<2874:TROIPS>2.0.CO;2, 1998.

McGill, M. J., Vaughan, M. A., Trepte, C. R., Hart, W. D., Hlavka, D. L., Winker, D. M., and Kuehn, R.: Airborne validation of spatial properties measured by the CALIPSO lidar, Journal of Geophysical Research Atmospheres, 112, 1–8, https://doi.org/10.1029/2007JD008768, 2007.

Menzel, W. P., Frey, R. A., and Baum, B. A.: Cloud Top Properties and Cloud Phase Algorithm Theoretical Basis Document Collection 006 Update, p. 73, 2015.

https://doi.org/10.5194/amt-2024-163
Preprint. Discussion started: 1 October 2024

Minnis, P., Trepte, Q. Z., Sun-Mack, S., Chen, Y., Doelling, D. R., Young, D. F., Spangenberg, D. A., Miller, W. F., Wielicki, B. A., Brown, R. R., Gibson, S. C., and Geier, E. B.: Cloud detection in nonpolar regions for CERES using TRMM VIRS and Terra and Aqua MODIS data, IEEE Transactions on Geoscience and Remote Sensing, 46, 3857–3884, https://doi.org/10.1109/TGRS.2008.2001351, 2008.

Mishchenko, M. I., Rossow, W. B., Macke, A., and Lacis, A.: Sensitivity of cirrus cloud albedo, bidirectional reflectance and optical thickness retrieval accuracy to ice particle shape, Journal of Geophysical Research, 101, 16 973–16 985, 1996.

Murino, L., Amato, U., Carfora, M. F., Antoniadis, A., Huang, B., Menzel, W. P., and Serio, C.: Cloud detection of modis multispectral images, Journal of Atmospheric and Oceanic Technology, 31, 347–365, https://doi.org/10.1175/JTECH-D-13-00088.1, 2014.

Musial, J. P., Hüsler, F., Sütterlin, M., Neuhaus, C., and Wunderle, S.: Daytime low stratiform cloud detection on AVHRR imagery, Remote Sensing, 6, 5124–5150, https://doi.org/10.3390/rs6065124, 2014.

M.Winker, D., Hostetler, C. A., Vaughan, M., and Omar, A.: CALIOP Algorithm Theoretical Basis Document Part 1 : CALIOP Instrument, and Algorithms Overview, 2006.

Oreopoulos, L., Cho, N., and Lee, D.: New Insights about Cloud Vertical Structure from CloudSat and CALIPSO observations, Journal of Geophysical Research Atmospheres, 122, 9280–9300, https://doi.org/10.1002/2017JD026629.New, 2017.

Orlowsky, B., Bothe, O., Fraedrich, K., Gerstengarbe, F. W., and Zhu, X.: Future climates from bias-bootstrapped weather analogs: An application to the Yangtze River basin, Journal of Climate, 23, 3509–3524, https://doi.org/10.1175/2010JCLI3271.1, 2010.

Pandit, A. K., Gadhavi, H. S., Venkat Ratnam, M., Raghunath, K., Rao, S. V. B., and Jayaraman, A.: 16 year climatology of cirrus clouds over a tropical station in southern India using ground and space-based lidar observations, Atmospheric Chemistry and Physics Discussions, 15, 15 791–15 830, https://doi.org/10.5194/acpd-15-15791-2015, 2015.

Ramanathan, V., Cess, R., Harrison, E., Minnis, P., Barkstrom, B., Ahmad, E., and Hartmann, D.: Cloud-Radiative Forcing and Climate : Results, Science, 243, 57–63, 1989.

Rossow, W. B. and Schiffer, R. A.: ISCCP Cloud Data Product, 72, 1991.

Sassen, K., Wang, Z., and Liu, D.: Global distribution of cirrus clouds from CloudSat/cloud-aerosol lidar and infrared pathfinder satellite observations (CALIPSO) measurements, Journal of Geophysical Research Atmospheres, 114, 1–12, https://doi.org/10.1029/2008JD009972, 2008.

Stanski, H., Wilson, L., and Burrows, W.: Survey of Common Verification Methods in Meteorology, Tech. rep., ISBN 9788578110796, ISSN 1098-6596, 1989.

Stephens, G. L. and Webster, P. J.: Clouds and Climate: Sensitivity of Simple Systems, Journal of Atmospheric Sciences, 38, 235–247, 1981.

Stephens, G. L., Tsay, S. C., Stackhouse, P. W., and Flatau, P. J.: The relevance of the microphysical and radiative properties of cirrus clouds to climate and climatic feedback, https://doi.org/10.1175/1520-0469(1990)047<1742:trotma>2.0.co;2, 1990.

Stephens, G. L., Winker, D., Pelon, J., Trepte, C., Vane, D., Yuhas, C., L'Ecuyer, T., and Lebsock, M.: Cloudsat and calipso within the a-train: Ten years of actively observing the earth system, Bulletin of the American Meteorological Society, 99, 569–581, https://doi.org/10.1175/BAMS-D-16-0324.1, 2018.

Stordal, F., Myhre, G., Stordal, E. J., Rossow, W. B., Lee, D. S., Arlander, D. W., and Svendby, T.: Is there a trend in cirrus cloud cover due to aircraft traffic?, Atmospheric Chemistry and Physics, 5, 2155–2162, https://doi.org/10.5194/acp-5-2155-2005, 2005.

Stubenrauch, C. J., Cros, S., Guignard, A., and Lamquin, N.: A 6-year global cloud climatology from the Atmospheric InfraRed Sounder AIRS and a statistical analysis in synergy with, Atmospheric Chemistry and Physics Discussions, 15, https://doi.org/10.5194/acp-10-7197-2010, 2010.

https://doi.org/10.5194/amt-2024-163
Preprint. Discussion started: 1 October 2024

Sun-Mack, S., Minnis, P., Chen, Y., Kato, S., Yi, Y., Gibson, S. C., Heck, P. W., Winker, and M., D.: Regional apparent boundary layer lapse rates determined from CALIPSO and MODIS data for cloud-height determination, Journal of Applied Meteorology and Climatology, 53, 990–1011, https://doi.org/10.1175/JAMC-D-13-081.1, 2014.

Tang, H., Yu, K., Hagolle, O., Jiang, K., Geng, X., and Zhao, Y.: A cloud detection method based on a time series of MODIS surface reflectance images, International Journal of Digital Earth, 6, 157–171, https://doi.org/10.1080/17538947.2013.833313, 2013.

Thorsen, T. J., Fu, Q., Comstock, J. M., Sivaraman, C., Vaughan, M. A., Winker, D. M., and Turner, D. D.: Macrophysical properties of tropical cirrus clouds from the CALIPSO satellite and from ground-based micropulse and Raman lidars, Journal of Geophysical Research Atmospheres, 118, 9209–9220, https://doi.org/10.1002/jgrd.50691, 2013.

Vaughan, M. A., Powell, K. A., Kuehn, R. E., Young, S. A., Winker, D. M., Hostetler, C. A., Hunt, W. H., Liu, Z., Mcgill, M. J., and Getzewich, B. J.: Fully automated detection of cloud and aerosol layers in the CALIPSO lidar measurements, Journal of Atmospheric and Oceanic Technology, 26, 2034–2050, https://doi.org/10.1175/2009JTECHA1228.1, 2009.

Wang, T., Fetzer, E. J., Wong, S., Kahn, B. H., and Yue, Q.: Validation of MODIS cloud mask and multilayer fl ag using CloudSat-CALIPSO cloud profiles and a cross-reference of their cloud classifications, Journal of geophysical research, 121, https://doi.org/10.1038/175238c0, 2016.

Wilks, D. S., Neumann, C. J., and Lawrence, M. B.: Statistical extension of the National Hurricane Center 5-day forecasts, Weather and Forecasting, 24, 1052–1063, https://doi.org/10.1175/2009WAF2222189.1, 2009.

WMO: International Cloud Atlas, Volume I: Manual on the Observation of Clouds and Other Meteors, ISBN 9263104077, https://doi.org/10.2307/1550553, 1977.

Wylie, D. P., Menzel, W. P., Woolf, H. M., and Strabala, K. I.: Four Years of Global Cirrus Cloud Statistics Using HIRS, Journal of Climate, 7, 1972–1986, 1994.

Xie, Y., Qu, J. J., and Xiong, X.: Improving the CALIPSO VFM product with Aqua MODIS measurements, Remote Sensing Letters, 1, 195–203, https://doi.org/10.1080/01431161003720387, 2010.

Zhang, Y., Laube, M., and Raschke, E.: Numerical simulations of cirrus properties, Contributions to Atmospheric Physics, 67, 109–120, 1994.

Zhang, Y., MacKe, A., and Albers, F.: Effect of crystal size spectrum and crystal shape on stratiform cirrus radiative forcing, Atmospheric Research, 52, 59–75, https://doi.org/10.1016/S0169-8095(99)00026-5, 1999.